



AMS

American Meteorological Society

Supplemental Material

Journal of Hydrometeorology

Influence of Underlying Surface Datasets on Simulated Hydrological Variables in the
Xijiang River Basin

<https://doi.org/10.1175/JHM-D-22-0095.1>

© Copyright 2023 American Meteorological Society (AMS)

For permission to reuse any portion of this work, please contact permissions@ametsoc.org. Any use of material in this work that is determined to be “fair use” under Section 107 of the U.S. Copyright Act (17 USC §107) or that satisfies the conditions specified in Section 108 of the U.S. Copyright Act (17 USC §108) does not require AMS’s permission. Republication, systematic reproduction, posting in electronic form, such as on a website or in a searchable database, or other uses of this material, except as exempted by the above statement, requires written permission or a license from AMS. All AMS journals and monograph publications are registered with the Copyright Clearance Center (<https://www.copyright.com>). Additional details are provided in the AMS Copyright Policy statement, available on the AMS website (<https://www.ametsoc.org/PUBSCopyrightPolicy>).

Supplementary

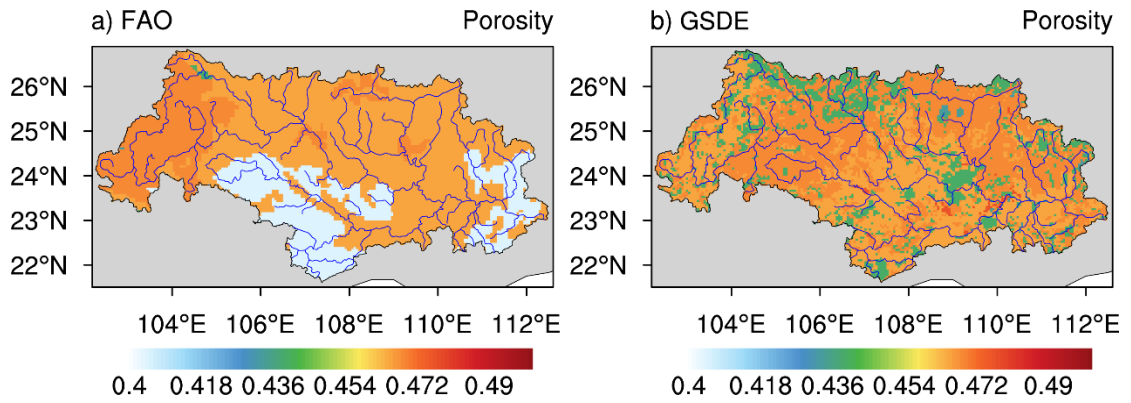


Fig. S1 Spatial patterns of porosity.

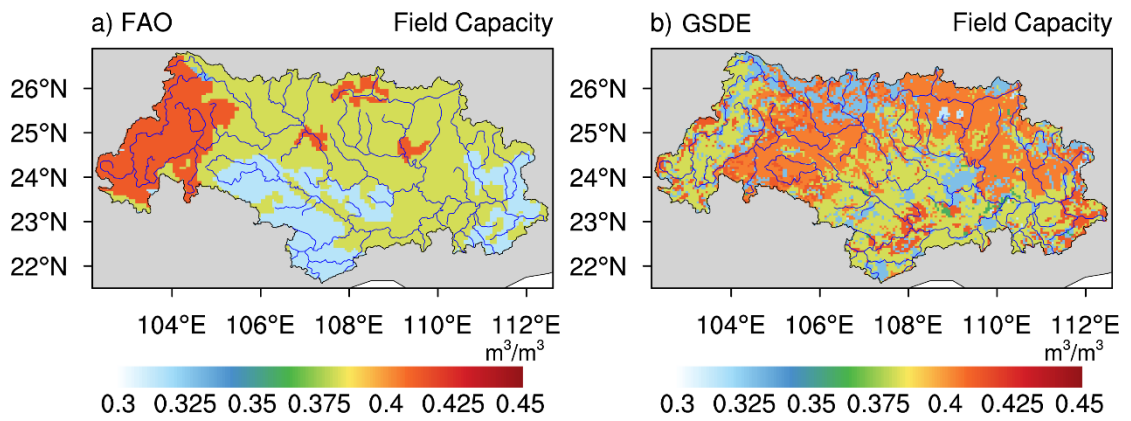


Fig. S2 Spatial patterns of field capacity (m^3/m^3).

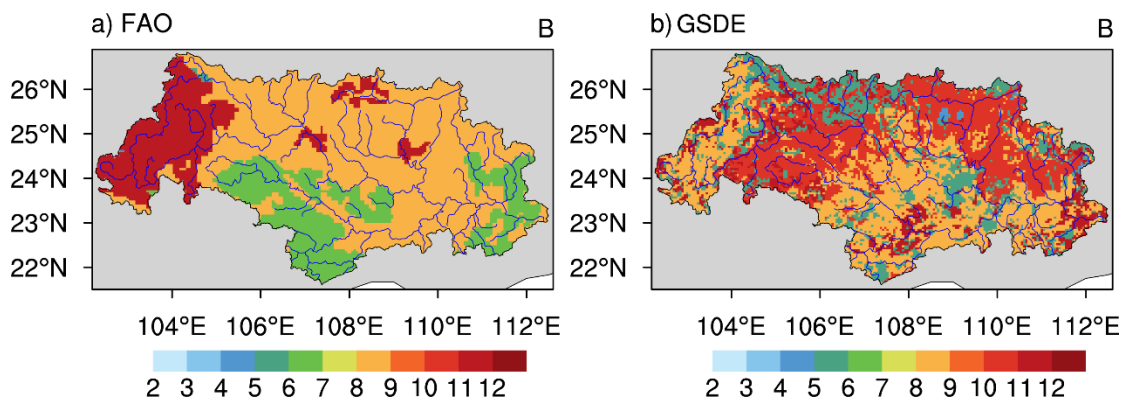


Fig. S3 Spatial patterns of parameter B.

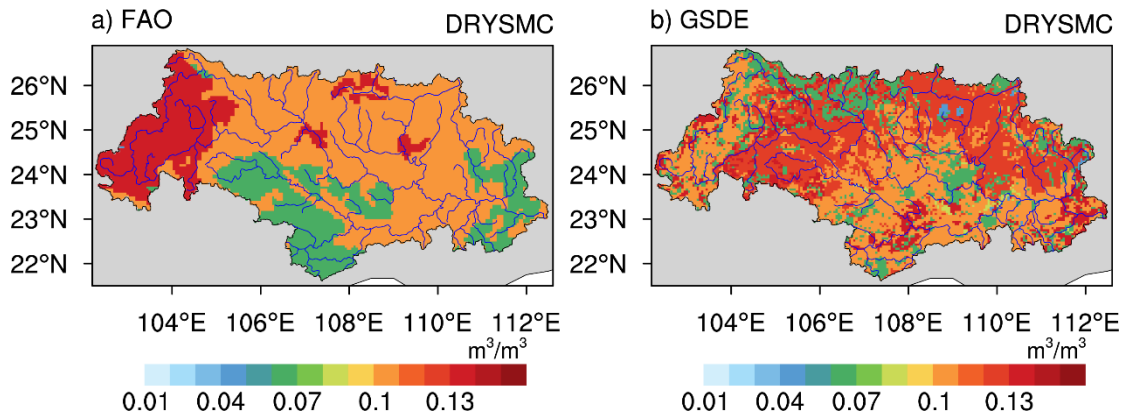


Fig. S4 Spatial patterns of dry soil moisture threshold (m^3/m^3) at which direct evaporation from top soil layer ends.

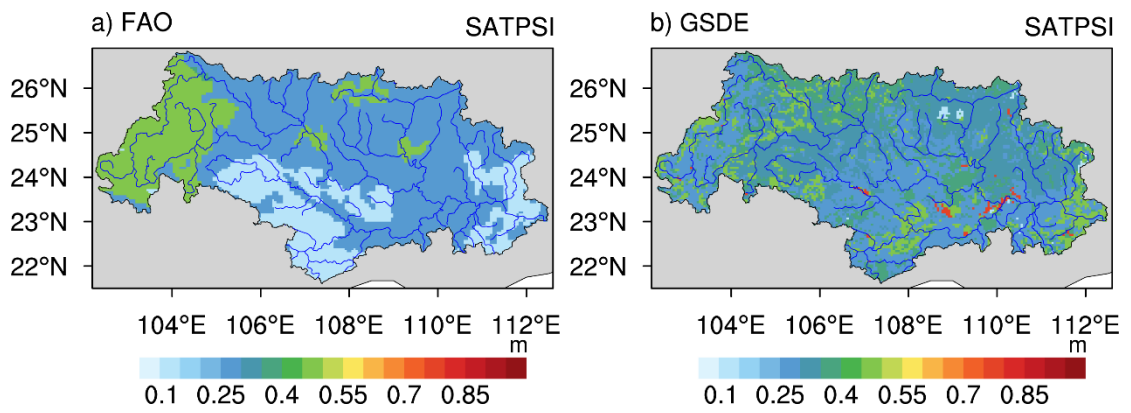


Fig. S5 Spatial patterns of saturation soil matric potential (m).

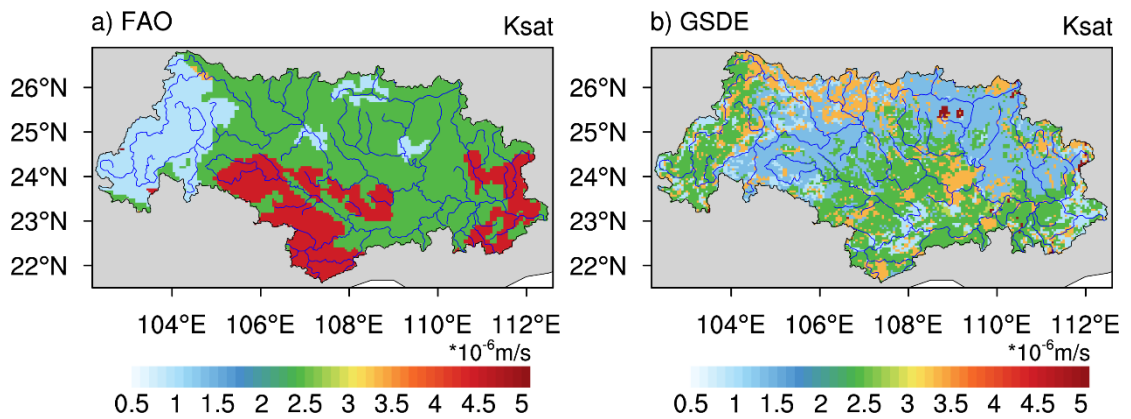


Fig. S6 Spatial patterns of saturation soil conductivity ($\ast 10^{-6}\text{m/s}$).

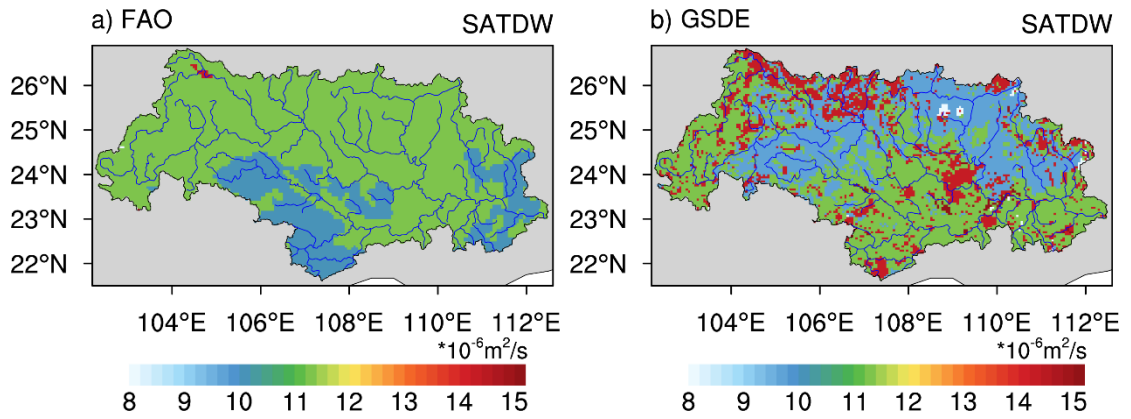


Fig. S7 Spatial patterns of saturation soil diffusivity ($\times 10^{-6} \text{m}^2/\text{s}$).

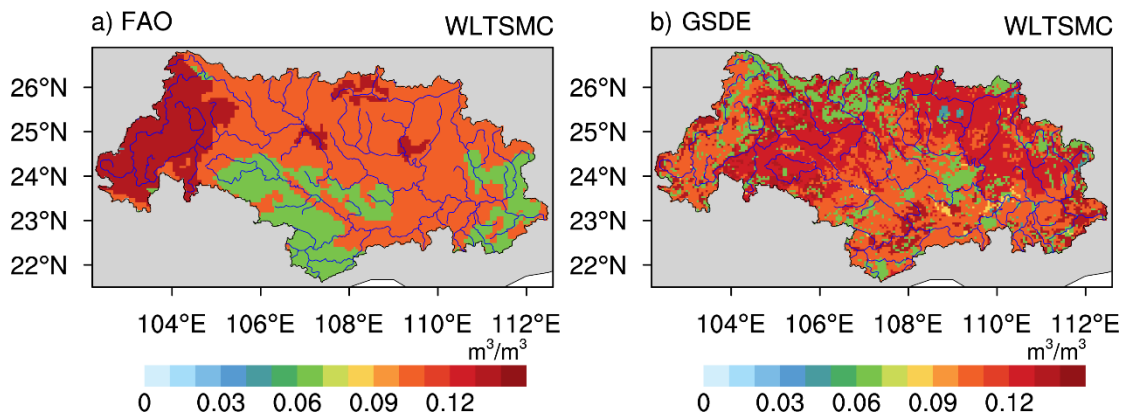


Fig. S8 Spatial patterns of wilting point (m^3/m^3) soil moisture.

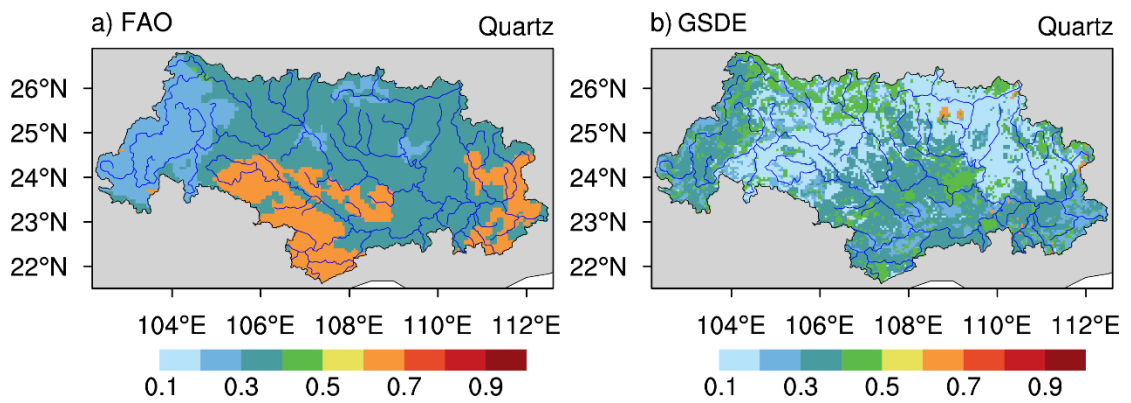


Fig. S9 Spatial patterns of soil quartz content.

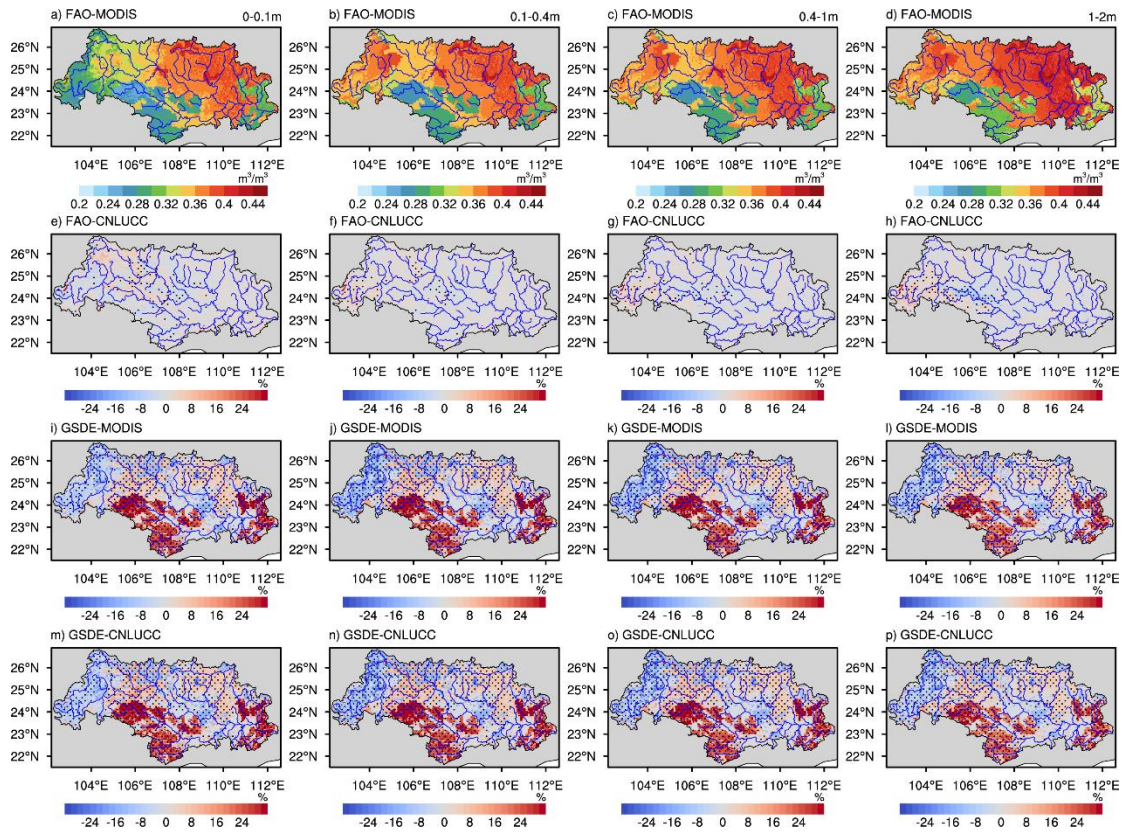


Fig. S10 Spring mean soil moisture (m^3/m^3) at different depths in FAO-MODIS (a–d), and annual mean soil moisture at different depths in other cases relative change to the spring mean soil moisture of FAO-MODIS (e–p). The dots represent statistically significant differences in monthly values at the 95% confidence interval.

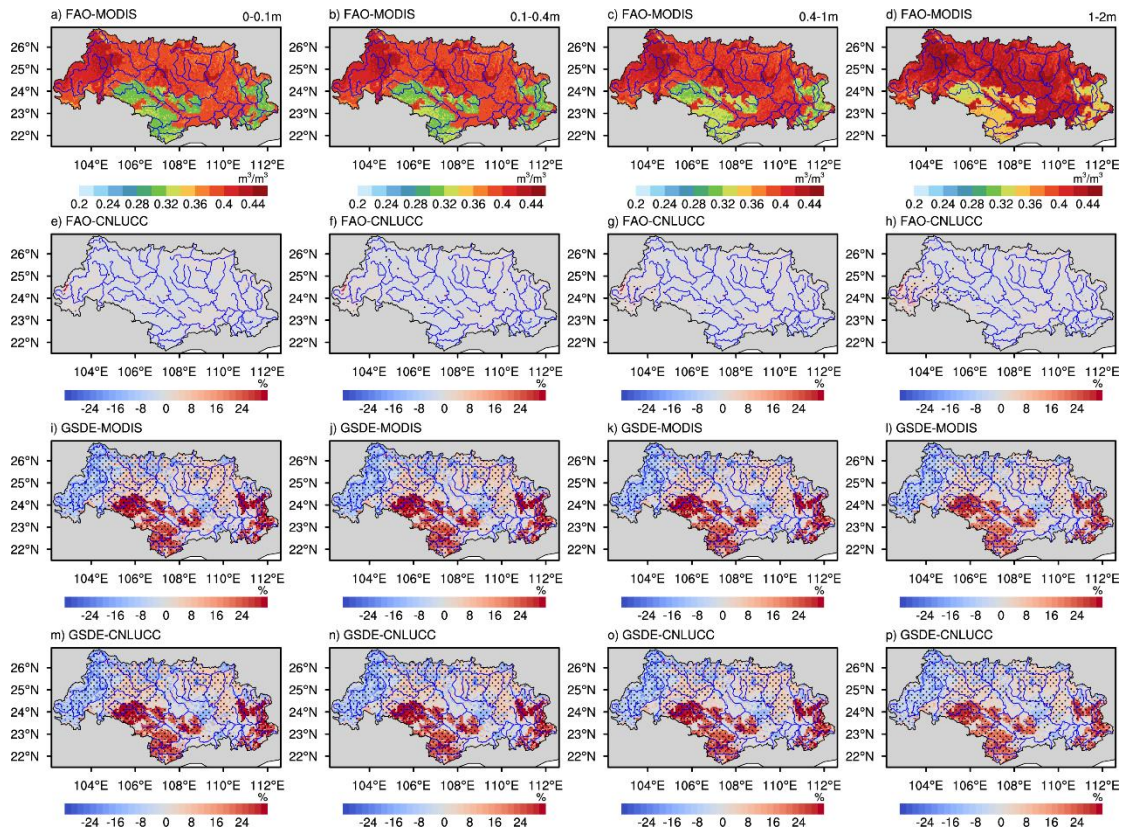


Fig. S11 Summer mean soil moisture (m^3/m^3) at different depths in FAO-MODIS (a–d), and annual mean soil moisture at different depths in other cases relative change to the summer mean soil moisture of FAO-MODIS (e–p). The dots represent statistically significant differences in monthly values at the 95% confidence interval.

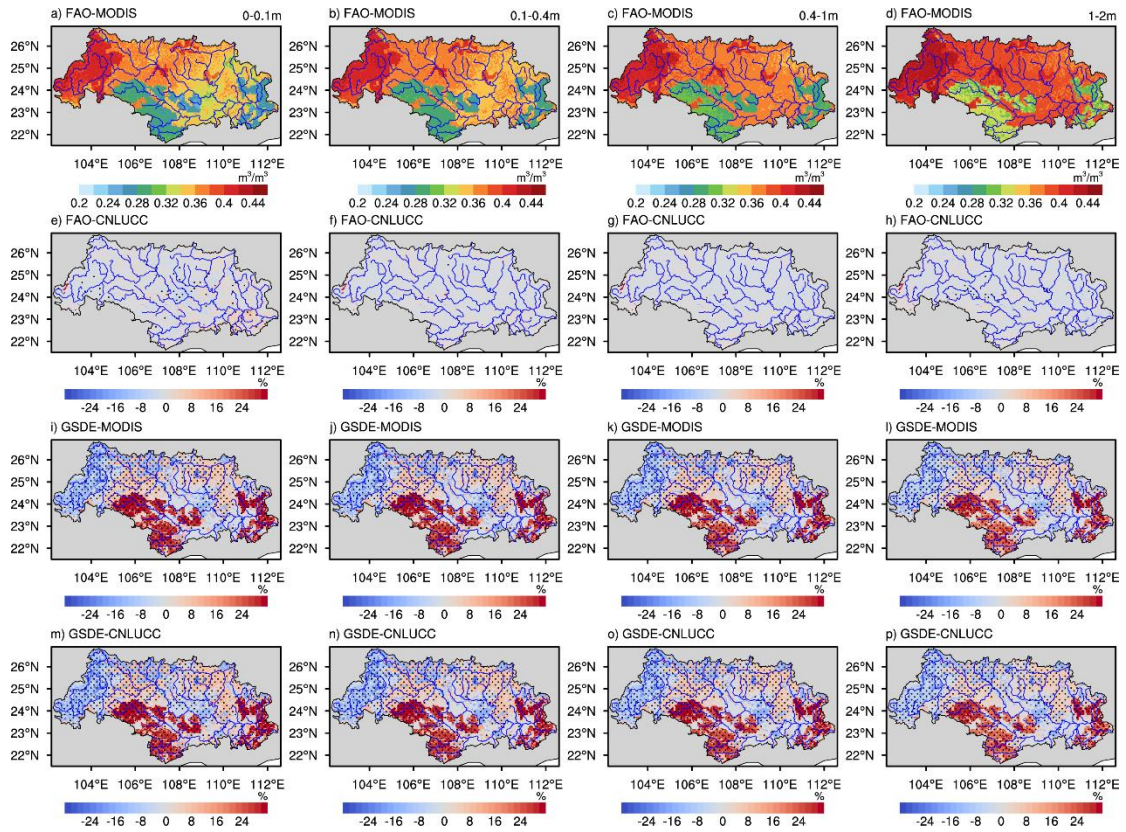


Fig. S12 Autumn mean soil moisture (m^3/m^3) at different depths in FAO-MODIS (a–d), and annual mean soil moisture at different depths in other cases relative change to the autumn mean soil moisture of FAO-MODIS (e–p). The dots represent statistically significant differences in monthly values at the 95% confidence interval.

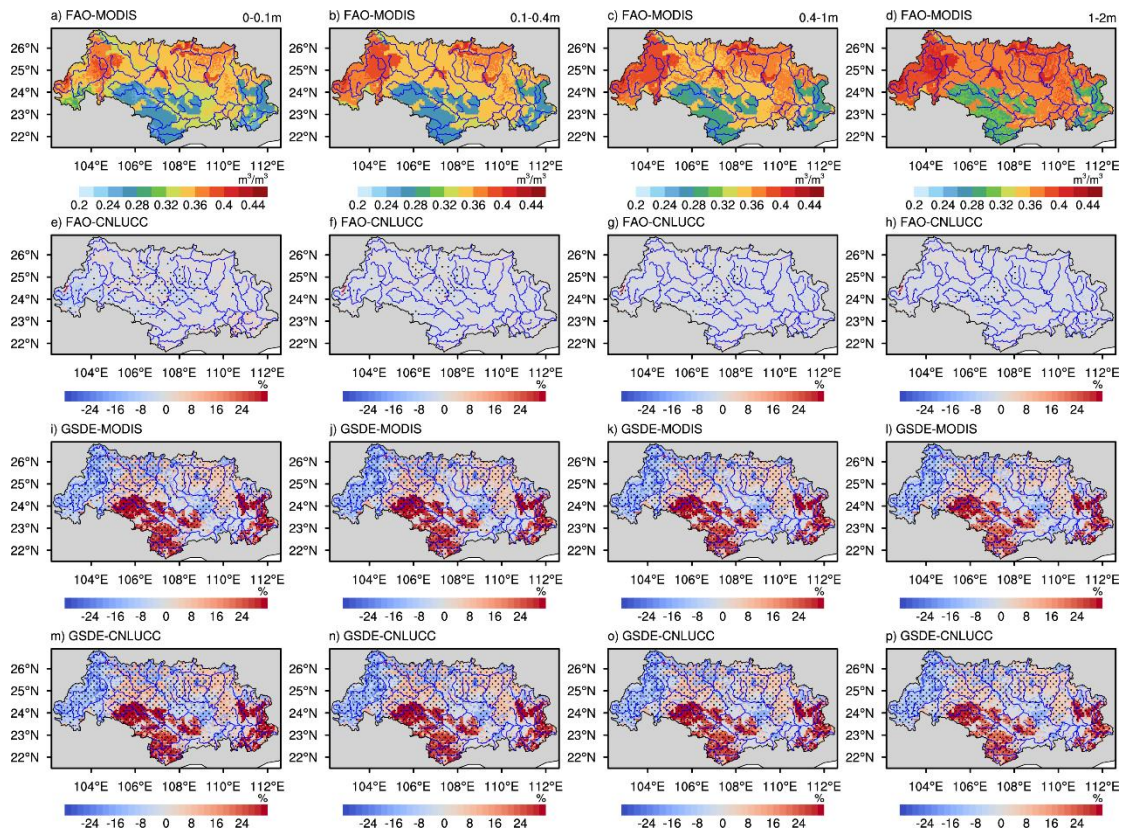


Fig. S13 Winter mean soil moisture (m^3/m^3) at different depths in FAO-MODIS (a–d), and annual mean soil moisture at different depths in other cases relative change to the winter mean soil moisture of FAO-MODIS (e–p). The dots represent statistically significant differences in monthly values at the 95% confidence interval.

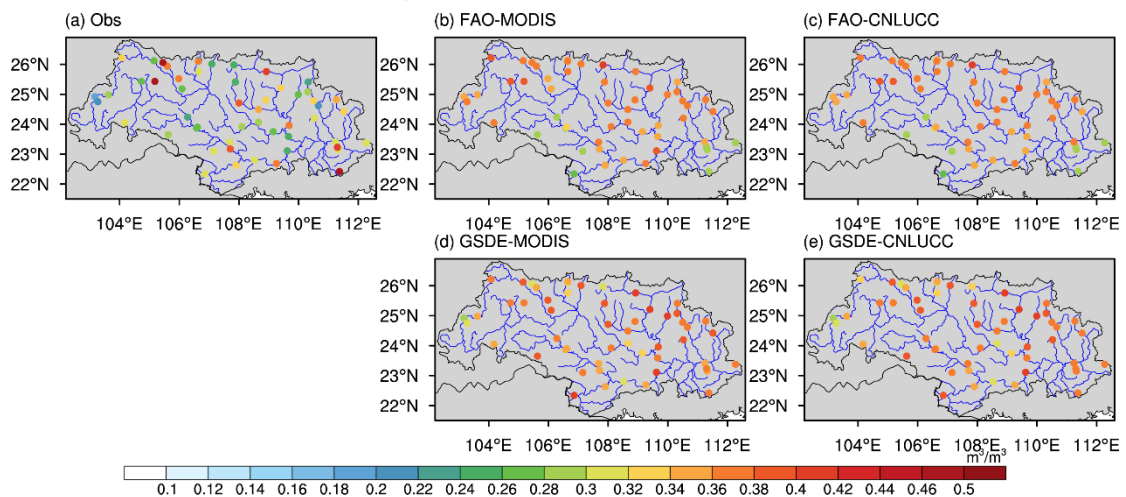


Fig. S14 Spatial distribution of annual mean (a) observed and (b–e) simulated soil moisture (m^3/m^3).

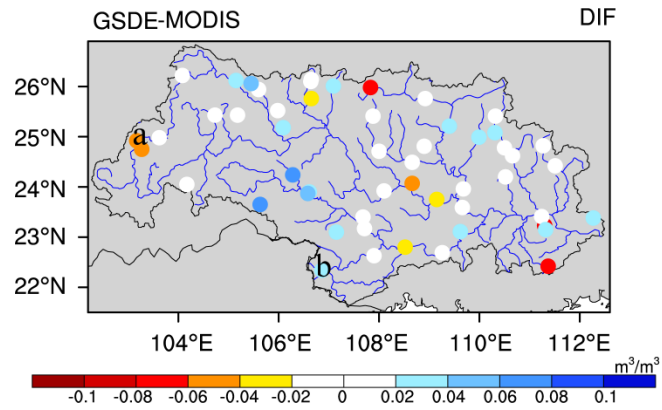


Fig. S15 The spatial distribution of the differences of RMSE (m^3/m^3) between GSDE-MODIS and FAO-MODIS, where the marked stations are the stations that are used in Fig. S16.

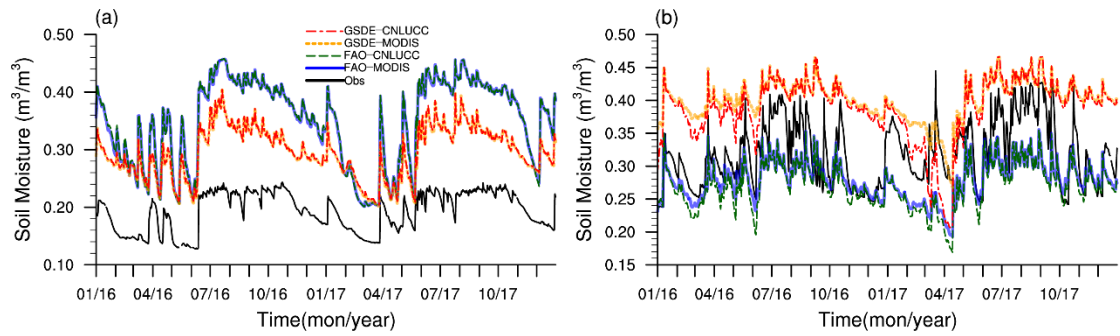


Fig. S16 The daily soil moisture (m^3/m^3) time series of the four cases and observation at two stations (stations marked in Fig. S15) in 2016-2017.